Investigation of Negative-Sequence Injection Capability of Cascaded H-Bridge Converters in Star and Delta Configuration

Ehsan Behrouzian, *Student Member, IEEE*, and Massimo Bongiorno, *Senior Member, IEEE*

***Abstract*—The aim of this paper is to investigate the ability of cascaded H-bridge STATic COMpensator in star and delta configuration to exchange negative-sequence current with the connecting grid. Zero-sequence voltage for the star and zero-sequence current for the delta configuration are utilized to guarantee dc-capacitor voltage balancing. A general solution for the required zero-sequence voltage/current for any kind of unbalanced condition is provided. The obtained solutions show that a singularity for both configurations exists under specific conditions, leading to infinite zero-sequence requirement. In case of star configuration, this singularity occurs when the amplitude of the positive- and negative-sequence components of the current output of the converter are equal. Analogously, the singularity for the delta configuration occurs when the amplitude of the positive- and negative-sequence components of the voltage at the converter terminals are equal. This singularity impacts the ratings of the system and imposes a limitation in the utilization of the compensator for unbalance compensation purposes, both in industrial and utility applications. Experimental results are presented to validate the theoretical analysis.**

***Index Terms*—Cascaded multilevel converter, dc-voltage balancing, FACTS, STATic COMpensator (STATCOM), unbalanced conditions.**

I. Introduction

THE actual trend in the market clearly indicates that voltage source converter (VSC)-based reactive power compensators will be more and more utilized in the power systems, both for utility and industrial applications. When connected in shunt with the grid, the VSC system (also named STATic COMpensator, STATCOM) has a smaller footprint than the equivalent thyristor-based solution (or static var compensator), better dynamic performance and increased robustness in case of connection to weak grids.

The modular multilevel converter (MMC) is considered as one of the most attractive topologies available for grid applications and in the last decade it has gained more and more attention both from the research community and from the manufacturers [1].

Manuscript received November 16, 2015; revised February 23, 2016; accepted April 12, 2016. Date of publication April 14, 2016; date of current version November 11, 2016. Recommended for publication by Associate Editor H.-P. Nee. This work was supported by ABB.

The authors are with the Department of Energy and Environment, Division of Electric Power Engineering, Chalmers University of Technology, Gothenburg 41296, Sweden (e-mail: ehsan.behrouzian@chalmers.se; massimo.bongiorno@chalmers.se).

Color versions of one or more of the figures in this paper are available online at http://ieeexplore.ieee.org.

Digital Object Identifier 10.1109/TPEL.2016.2554322

Among the MMCs family, the cascaded H-bridge (CHB) converter is one of the most interesting solutions for STATCOM applications [2]. Since the number of modules, or cells, is proportional to the ac voltage level at the connection point, the system is scalable and, if needed, allows transformerless connection to the grid [3]. For this converter topology, the phase legs can be connected either in delta or in star, depending on the specific application. The main disadvantage with CHB converters for grid applications is the lack of a common dc link and thereby the difficulty in exchanging energy between the phase legs. This is even more challenging in case of unbalanced grids, where countermeasures must be taken in order to preserve the balancing of the capacitors, thus avoiding drifting of the dc-link voltages. However, these solutions will have an impact on the overall rating of the converter.

In particular, in case of star-connected CHB-STATCOM, when the system is exchanging negative-sequence current with the grid, a zero-sequence voltage must be introduced in the output phase voltage of the converter to guarantee capacitor balancing, resulting in a movement of the floating Y-point of the converter [4]–[7]. This leads to the need for an increased number of series-connected cells in order to realize the required phase voltage. On the other hand, the delta configuration allows negative-sequence compensation by letting a zero-sequence current circulate inside the delta [8], which increases the required current rating for the compensator [9]–[11].

In the work presented in [12] and [13], the star-connected CHB is considered as the most suitable configuration for positive-sequence reactive power control, typically for voltage regulation purpose and, more in general, for utility applications; on the other hand, delta configuration is considered to be the best solution for applications where negative sequence is required, as it is the case for industrial applications (for example, flicker mitigation).

However, requirements from transmission system operators are changing and start to demand negative-sequence injection capability for the converters connected to their grid [14]. Furthermore, the delta configuration can present limitations in injecting negative-sequence current in case of weak grids, where both load current and voltage are unbalanced, or under unbalanced fault conditions [13]. For this reason, it is of high importance to investigate the limits in terms of negative-sequence compensation for this kind of controllers.

The aim of this paper is to investigate the ability of both star and delta connected CHB-STATCOM to exchange negative-sequence current with the grid. A general solution for the

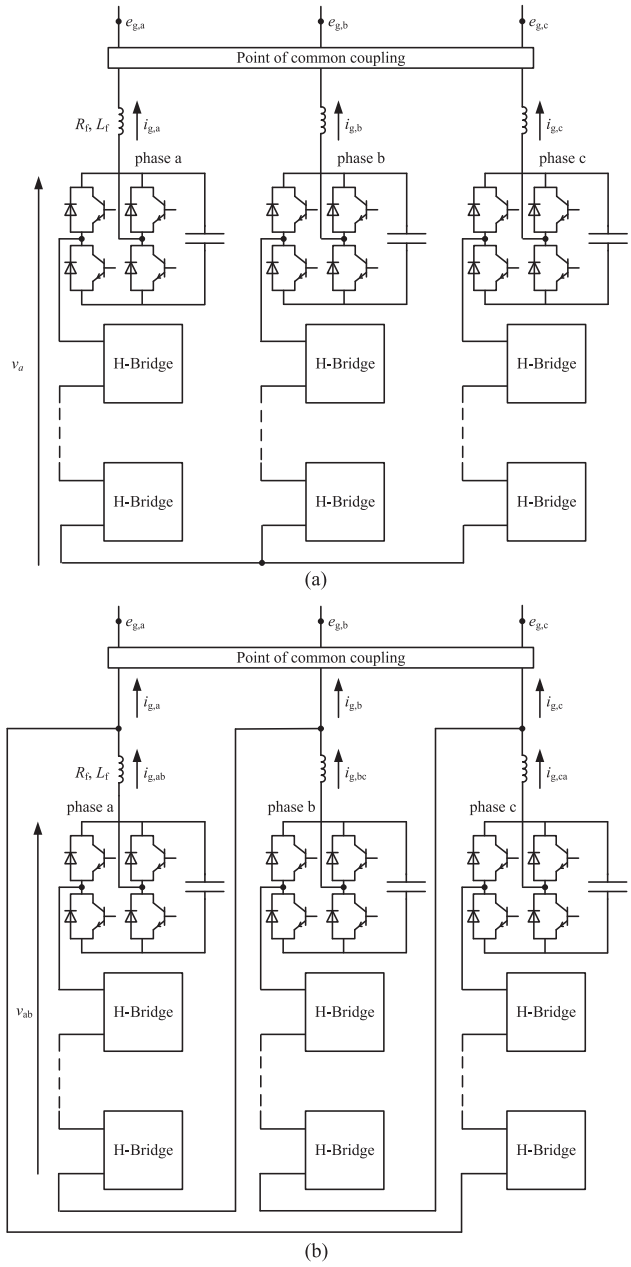

Fig. 1. CHB multilevel converter. (a) star configuration, (b) delta configuration.

required zero-sequence voltage and current under any unbalanced condition will be derived. It will be shown that both configurations exhibit a singularity in the solution of the zero-sequence component, which in turn limits the operational range of the compensator under unbalanced conditions. Theoretical analysis is validated via experimental results for both delta and star configurations.

II. Impact of Unbalanced Conditions on Active Power Distribution

Fig. 1 shows the line diagram of a CHB-STATCOM, both in delta and star configurations. Each phase consists of N H-bridge converters (or cells) connected in series. In case of star configuration, the converter is connected to the grid through three single-phase filter reactors to handle the voltage difference between the converter and the grid. For the delta configuration, the filter reactor is typically connected inside the delta; in this way, the filter can handle the voltage difference between converter phases and limit the circulating current inside the delta.

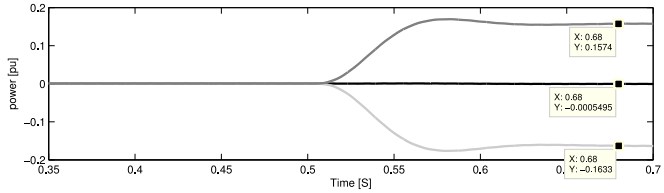

Fig. 2. Effect of unbalanced condition on active power at each phase of star configuration.

The active power in each phase (p_a, p_b, p_c) can be calculated by the inner product of the phase current and voltage. The resulting power will contain both a constant $(P_{\rm ava}, P_{\rm avb}, P_{\rm avc})$ and an oscillating term (denoted as $p_{\rm osca}, p_{\rm oscb}, p_{\rm oscc}$), which oscillates at twice the grid frequency

$$p_i = P_{\rm avi} + p_{\rm osci}, \qquad i = a, b, c. \tag{1}$$

Observe that if the system losses are neglected, the sum of the average terms in the phase active power is always zero.

In order to show the effect of an unbalanced condition on the phase active powers, the star-connected CHB-STATCOM is here simulated when injecting a negative-sequence current in the grid. For this simulation, the dc-link capacitors are replaced by ideal dc sources. Fig. 2 shows the active power flowing in each phase of system. For clarity of the illustration, the plotted powers are low-pass filtered in order to remove the double-frequency component. The grid is balanced and the STATCOM is injecting 0.9 p.u. positive-sequence current in the grid. At $t = 0.5$ s the negative-sequence current is stepped from 0 to 0.4 p.u. It is clearly possible to observe from the figure that under this condition, different active powers will flow in each phase leg; this would lead to diverging dc-capacitor voltages in the phase legs. Notice that, under unbalanced condition, the sum of the three-phase power is still zero. The same problem will occur for the delta configuration.

III. Control Solution Under Unbalanced Conditions

The control system of CHB-STATCOM must guarantee that the active power is equally distributed among the phase legs, in order to compensate for the system losses and keep the charge of the dc capacitors. Considering the star configuration, a zero-sequence voltage can be added to all phases to fulfill this requirement. Assuming an unbalanced condition of the system and with reference to Fig. 1(a), the phasors of the converter phase voltage and current for phase a can be written as

$$\begin{aligned} \overline{V}_a &= V^+ e^{j\theta_v^+} + V^- e^{j\theta_v^-} + V_0 e^{j\theta_{v0}} \\ \overline{I}_{g,a} &= I^+ e^{j\delta_i^+} + I^- e^{j\delta_i^-} \end{aligned} \tag{2}$$

with

1) V^-, V^+: Negative- and positive-sequence voltage phasor amplitude.
2) θ_v^-, θ_v^+: Negative- and positive-sequence voltage phasor angle.
3) I^-, I^+: Negative- and positive-sequence current phasor amplitude.
4) δ_i^-, δ_i^+: Negative- and positive-sequence current phasor angle.

Analogous relations hold for the other two phases of the converter.

The introduction of a zero-sequence voltage allows two degrees of freedom, in terms of amplitude (V_0) and angle (θ_{v0}). The goal is to find a suitable value for V_0 and θ_{v0} to remove the interaction between the sequence components and, thus, provide an uniform active power distribution among phases. Considering phases a and b and considering zero-sequence voltage injection, the total active power can be written as

$$\begin{aligned}
P_a &= \frac{V^+I^+}{2}\cos(\theta_v^+ - \delta_i^+) + \frac{V^-I^-}{2}\cos(\theta_v^- - \delta_i^-) \\
&\quad + \frac{V^+I^-}{2}\cos(\theta_v^+ - \delta_i^-) + \frac{V^-I^+}{2}\cos(\theta_v^- - \delta_i^+) \\
&\quad + \frac{V_0I^-}{2}\cos(\theta_{v_0} - \delta_i^-) + \frac{V_0I^+}{2}\cos(\theta_{v_0} - \delta_i^+) \\
P_b &= \frac{V^+I^+}{2}\cos(\theta_v^+ - \delta_i^+) + \frac{V^-I^-}{2}\cos(\theta_v^- - \delta_i^-) \\
&\quad + \frac{V^+I^-}{2}\cos(\theta_v^+ - \delta_i^- - \frac{4\pi}{3}) \\
&\quad + \frac{V^-I^+}{2}\cos(\theta_v^- - \delta_i^+ + \frac{4\pi}{3}) \\
&\quad + \frac{V_0I^-}{2}\cos(\theta_{v_0} - \delta_i^- - \frac{2\pi}{3}) \\
&\quad + \frac{V_0I^+}{2}\cos(\theta_{v_0} - \delta_i^+ + \frac{2\pi}{3}). \qquad (3)
\end{aligned}$$

The first two terms in (3) indicate the active power expressions associated to the positive- and negative-sequence components. These terms are equal in all phases and can be controlled through the overall dc-link voltage controller, as it will be shown in Section IV-B. The third and fourth term denote the active power generated by the interaction between positive- and negative-sequence components; this interaction is responsible for the uneven power distribution between the phases. Finally, the last two terms in (3) are the active power terms generated by the zero-sequence voltage injection. Two main components can be identified in (3), an active power component that is common among the phases ($P_{\rm com}$) and a component caused by the interaction between the different sequences ($P_{\rm dis}$)

$$\begin{aligned}
P_{\rm com} &= \frac{V^+I^+}{2}\cos(\theta_v^+ - \delta_i^+) + \frac{V^-I^-}{2}\cos(\theta_v^- - \delta_i^-) \\
P_{\rm disa} &= \frac{V^+I^-}{2}\cos(\theta_v^+ - \delta_i^-) + \frac{V^-I^+}{2}\cos(\theta_v^- - \delta_i^+) \\
&\quad + \frac{V_0I^-}{2}\cos(\theta_{v_0} - \delta_i^-) + \frac{V_0I^+}{2}\cos(\theta_{v_0} - \delta_i^+) \\
P_{\rm disb} &= \frac{V^+I^-}{2}\cos(\theta_v^+ - \delta_i^- - \frac{4\pi}{3}) \\
&\quad + \frac{V^-I^+}{2}\cos(\theta_v^- - \delta_i^+ + \frac{4\pi}{3}) \\
&\quad + \frac{V_0I^-}{2}\cos(\theta_{v_0} - \delta_i^- - \frac{2\pi}{3}) \\
&\quad + \frac{V_0I^+}{2}\cos(\theta_{v_0} - \delta_i^+ + \frac{2\pi}{3}). \qquad (4)
\end{aligned}$$

Under ideal conditions, the interaction between sequences is the only disturbing factor that leads to the uneven power distribution between the different phases. Therefore, calculating an appropriate zero-sequence voltage amplitude and phase that makes $P_{\rm disa} = P_{\rm disb} = 0$ will be sufficient to guarantee the balancing of the dc-capacitors voltages. However, in practical applications other factors (such as different components characteristics) will impact the active power flowing in the phase legs. Therefore, (4) can be solved for a general case to find the appropriate zero-sequence voltage to compensate any kind of power disturbance as well as interaction between negative and positive sequences. Let us introduce two new variables K_1 and K_2, defined as

$$\begin{aligned}
K_1 &= \frac{V^+I^-}{2}\cos(\theta_v^+ - \delta_i^-) + \frac{V^-I^+}{2}\cos(\theta_v^- - \delta_i^+) \\
K_2 &= \frac{V^+I^-}{2}\cos(\theta_v^+ - \delta_i^- - \frac{4\pi}{3}) \\
&\quad + \frac{V^-I^+}{2}\cos(\theta_v^- - \delta_i^+ + \frac{4\pi}{3}). \qquad (5)
\end{aligned}$$

Expanding the cosine terms in (3), $P_{\rm disa}$ and $P_{\rm disb}$ can be rewritten as

$$\begin{aligned}
P_{\rm disa} &= K_1 + V_0\cos(\theta_{v_0})\Big[\underbrace{\frac{I^-}{2}\cos(\delta_i^-) + \frac{I^+}{2}\cos(\delta_i^+)}_{K_3 = \frac{1}{2}{\rm Re}[\overline{I}_{g,a}]}\Big] \\
&\quad + V_0\sin(\theta_{v_0})\Big[\underbrace{\frac{I^-}{2}\sin(\delta_i^-) + \frac{I^+}{2}\sin(\delta_i^+)}_{K_4 = \frac{1}{2}{\rm Im}[\overline{I}_{g,a}]}\Big] \\
P_{\rm disb} &= K_2 \\
&\quad + V_0\cos(\theta_{v_0})\Big[\underbrace{\frac{I^-}{2}\cos(\delta_i^- \frac{2\pi}{3}) + \frac{I^+}{2}\cos(\delta_i^+ - \frac{2\pi}{3})}_{K_5 = \frac{1}{2}{\rm Re}[\overline{I}_{g,b}]}\Big] \\
&\quad + V_0\sin(\theta_{v_0})\Big[\underbrace{\frac{I^-}{2}\sin(\delta_i^- + \frac{2\pi}{3}) + \frac{I^+}{2}\sin(\delta_i^+ - \frac{2\pi}{3})}_{K_6 = \frac{1}{2}{\rm Im}[\overline{I}_{g,b}]}\Big]. \qquad (6)
\end{aligned}$$

The set of equations above can be simplified in order to isolate the terms that involves the zero-sequence voltage as

$$\begin{aligned}
P_{\rm disa} - K_1 &= K_3V_0\cos(\theta_{v_0}) + K_4V_0\sin(\theta_{v_0}) \\
P_{\rm disb} - K_2 &= K_5V_0\cos(\theta_{v_0}) + K_6V_0\sin(\theta_{v_0}) \qquad (7)
\end{aligned}$$

where the different terms have the meaning as indicated in (6). Solving (7), the phase angle and amplitude of the zero-sequence voltage are [15]

$$\begin{aligned}\tan\theta_{v_0} &= \frac{(P_{\rm disb}-K_2)K_3-(P_{\rm disa}-K_1)K_5}{(P_{\rm disa}-K_1)K_6-(P_{\rm disb}-K_2)K_4}\\ V_0 &= \frac{P_{\rm disa}-K_1}{K_3\cos(\theta_{v_0})+K_4\sin(\theta_{v_0})}\\ &= \frac{P_{\rm disb}-K_2}{K_5\cos(\theta_{v_0})+K_6\sin(\theta_{v_0})}.\end{aligned} \tag{8}$$

As mentioned earlier, for the delta configuration a circulating current ($I_0 e^{j\delta_{i_0}}$) can be used to guarantee capacitor balancing. The circulating current flows only inside the delta, allowing power exchange between the phases without affecting the grid. Similar to the star configuration, the zero-sequence current allows two degrees of freedom in terms of its amplitude and phase. Assuming an unbalanced condition and with reference to Fig. 1(b), the converter phase voltage and current for phase a can be written as

$$\begin{aligned}\overline{V}_{\rm ab} &= V^+ e^{{\rm j}\theta_v^+} + V^- e^{j\theta_v^-}\\ \overline{I}_{g,{\rm ab}} &= I^+ e^{{\rm j}\delta_i^+} + I^- e^{j\delta_i^-} + I_0 e^{j\delta_{i_0}}.\end{aligned} \tag{9}$$

Following the same criteria adopted for the star case, the amplitude and phase of the zero-sequence current can be calculated as [15]

$$\begin{aligned}\tan\delta_{i_0} &= \frac{(P_{\rm disa}-K_{11})K_{15}-(P_{\rm disb}-K_{12})K_{13}}{(P_{\rm disb}-K_{12})K_{14}-(P_{\rm disa}-K_{11})K_{16}}\\ I_0 &= \frac{P_{\rm disa}-K_{11}}{K_{13}\cos(\delta_{i_0})+K_{14}\sin(\delta_{i_0})}\\ &= \frac{P_{\rm disb}-K_{12}}{K_{15}\cos(\delta_{i_0})+K_{16}\sin(\delta_{i_0})}\end{aligned} \tag{10}$$

where the different constant terms are defined as

$$\begin{aligned}K_{11} &= \frac{V^+I^-}{2}\cos(\theta_v^+-\delta_i^-)\\ &\quad+\frac{V^-I^+}{2}\cos(\theta_v^--\delta_i^+)\\ K_{12} &= \frac{V^+I^-}{2}\cos(\theta_v^+-\delta_i^--\frac{4\pi}{3})\\ &\quad+\frac{V^-I^+}{2}\cos(\theta_v^--\delta_i^++\frac{4\pi}{3})\\ K_{13} &= \frac{1}{2}{\rm Re}[\overline{V}_{\rm ab}], K_{14}=\frac{1}{2}{\rm Im}[\overline{V}_{\rm ab}]\\ K_{15} &= \frac{1}{2}{\rm Re}[\overline{V}_{\rm bc}], K_{16}=\frac{1}{2}{\rm Im}[\overline{V}_{\rm bc}].\end{aligned} \tag{11}$$

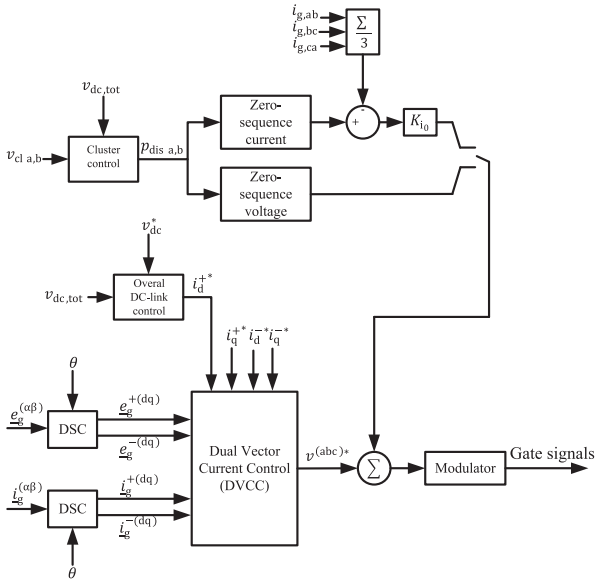

Fig. 3. Overall control block diagram.

IV. Control Design for Star and Delta

The aim of the implemented controller is to track both positive- and negative-sequence reference currents while at the same time control the dc-link voltages at a desired reference value. In this paper, the control system is implemented in the rotating dq-reference frame. The overall control block diagram is shown in Fig. 3. Three-phase quantities are transferred to the rotating dq-reference frame using a transformation angle θ, provided by a phase locked loop (PLL) [16], [17]. Positive- and negative-sequence components of the measured signals are estimated using delayed signal cancellation (DSC) technique [18] and are independently controlled using a dual vector current control (DVCC). A detailed description of the implemented DVCC and dc-link voltage control is provided in the following.

A. Dual Vector Current-Controller

The DVCC is constituted by two separate PI-based current controllers (CCs) implemented in the positive- and in the negative-synchronous reference frame, as shown in Fig. 4. Both grid voltage and filter current are separated into positive- and negative-sequence components and the controller tracks the corresponding reference currents. The CC outputs are the positive- and negative-sequence components of the reference output voltages in the corresponding dq-reference frame, given by

$$\begin{aligned}\underline{v}^{+({\rm dq})*} &= \underline{e}_g^{+({\rm dq})} + j\omega L_f \underline{i}_g^{+({\rm dq})} w\\ &\quad+\left(K_p+\frac{K_i}{s}\right)\left(\underline{i}^{+({\rm dq})*}-\underline{i}_g^{+({\rm dq})}\right)\\ \underline{v}^{-({\rm dq})*} &= \underline{e}_g^{-({\rm dq})} - j\omega L_f \underline{i}_g^{-({\rm dq})}\\ &\quad+\left(K_p+\frac{K_i}{s}\right)\left(\underline{i}^{-({\rm dq})*}-\underline{i}_g^{-({\rm dq})}\right)\end{aligned} \tag{12}$$

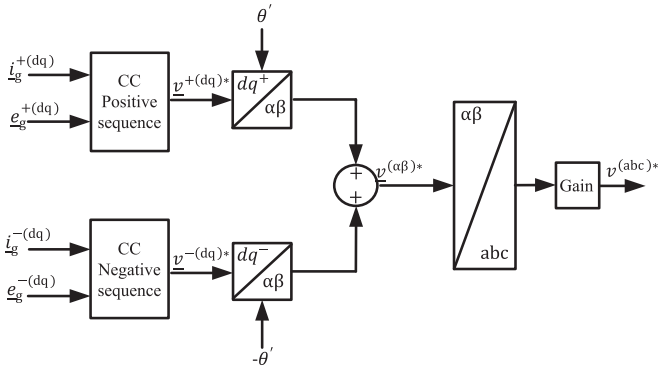

Fig. 4. Block diagram of DVCC. $\theta' = \theta$ and Gain $= 1$ for star case or $\theta' = \theta + \frac{\pi}{6}$ and Gain $= \sqrt{3}$ for delta case.

where $\underline{v}^{+(\mathrm{dq})*}$, $\underline{v}^{-(dq)*}$ and $\underline{e}_g^{+(\mathrm{dq})}$, $\underline{e}_g^{-(\mathrm{dq})}$ are the reference and grid dq positive- and negative-sequence voltages, respectively, while $\underline{i}^{+(\mathrm{dq})*}$, $\underline{i}^{-(\mathrm{dq})*}$ and $\underline{i}_g^{+(\mathrm{dq})}$, $\underline{i}_g^{-(\mathrm{dq})}$ are the positive- and negative-sequence components of the reference and actual grid currents, respectively. L_f is the filter inductance, ω is the angular frequency of grid voltage, and K_p and K_i are the controller proportional and integral gain, tuned as suggested in [19]. It should be noted that in (12) L_f should be replaced by $L_f/3$ for the delta configuration.

The obtained reference voltages are then transformed back to three-phase quantities and the converter switching pattern is obtained in the modulator block in Fig. 3 using sorting approach, as described in [20].

B. DC-Link Voltage Control

The dc-link voltage control comprises of two stages:

1) overall dc-link voltage control;
2) cluster voltage (defined as the average dc-link voltage in each phase) control.

The overall dc-link voltage control is responsible to provide sufficient power to maintain the charge of all dc capacitors in the three phases. Using a voltage-oriented dq transformation (d-axis aligned with the grid-voltage vector in steady state), the active power flow is controlled through the direct component of the positive-sequence current, as [19]

$$i_d^{+*} = K_{\mathrm{ov}}(v_{\mathrm{dc}}^{*^2} - v_{\mathrm{dc,tot}}^2) \tag{13}$$

where K_{ov} is the controller gain, $v_{\mathrm{dc,tot}}$ is the average voltage of all the dc-link voltages and v_{dc}^* is the reference value for the dc-link voltage.

The cluster voltage control calculates the amount of zero-sequence voltage from (8) for the star connection or zero-sequence current from (10) for the delta. This is achieved through the control of the disturbance power P_{disa} and P_{disb} as

$$\begin{aligned} p_{\mathrm{disa}} &= K_z(v_{\mathrm{dc,tot}}^2 - v_{\mathrm{cla}}^2) \\ p_{\mathrm{disb}} &= K_z(v_{\mathrm{dc,tot}}^2 - v_{\mathrm{clb}}^2) \end{aligned} \tag{14}$$

where k_z is a proportional gain and v_{cla} and v_{clb} are the cluster voltages of phase a and b, respectively.

Note that the zero-sequence voltage calculated for the star configuration can be directly added to the reference voltages output from the DVCC (see Fig. 3); for the delta configuration, instead, the zero-sequence voltage that leads to the desired current circulation is obtained through a proportional controller of gain K_{io} as

$$v_{i0} = K_{\mathrm{io}}\left(-\frac{(i_{a\Delta} + i_{b\Delta} + i_{c\Delta})}{3} + i_0\cos(\theta + \delta_{\mathrm{i0}})\right). \tag{15}$$

V. Operating Range of Star and Delta Under Unbalanced Conditions

The comparison between the delta and the star operating range is based on the required zero-sequence current and voltage to guarantee capacitor balancing under unbalanced conditions. According to (8) and based on the variables K_3 to K_6 in (6), it is possible to conclude that the star configuration is mainly sensitive to the amount of positive- and negative-sequence currents that the converter exchanges with the grid. Similarly, according to (10) and based on K_{13} to K_{16} defined in (11), the delta configuration is sensitive to the amplitude of the positive- and negative-sequence components of the voltage applied at the converter terminals.

To analyze the sensitivity of these two configurations, two case studies are here investigated: for the star configuration, it is assumed that the grid is balanced (thus, the grid voltage is only constituted by a positive-sequence component) while the converter is exchanging both positive- and negative-sequence current with the grid. For simplicity of the analysis, two operating conditions for the converter are here considered: the two current sequences have the same phase angle (for example, both positive- and negative-sequence currents are injected into the grid) or the current sequences are opposite in phase (for example, positive-sequence current is injected into the grid while the negative-sequence is absorbed by the compensator). In a dual situation, for the delta configuration it is assumed that the grid is unbalanced and the converter exchanges only positive-sequence current with the grid. The phase shift between the two sequence components of the voltage depends on a number of factors, for example the grid impedance and, in case of unbalance due to fault conditions, on the fault location and characteristic; here it is assumed that the phase shift between positive- and negative-sequence voltage is either equal to 0 or to π, in order to highlight the duality between the two configurations. It is also assumed that the filter impedance between the grid and converter is purely inductive and losses are neglected ($\delta^+ = \theta^+ \pm \frac{\pi}{2}$). Table I summarizes the different sequence components for the considered cases. The corresponding zero-sequence voltage and current are calculated using (8) and (10).

TABLE I
NEGATIVE- AND POSITIVE-SEQUENCE QUANTITIES WITH THEIR CORRESPONDING ZERO-SEQUENCE VOLTAGE OR CURRENT

	v^+, θ_v^+	v^-, θ_v^-	i^+, δ_i^+	i^-, δ_i^-	v_0 or i_0
star	$V^+, 0$	0,0	$I^+, \pm\frac{\pi}{2}$	$I^-, \pm\frac{\pi}{2}$	$\frac{A}{\sqrt{3}(I^{-2}-I^{+2})}$
star	$V^+, 0$	0,0	$I^+, \mp\frac{\pi}{2}$	$I^-, \pm\frac{\pi}{2}$	$\frac{A'}{\sqrt{3}(I^{-2}-I^{+2})}$
delta	$V^+, 0$	$V^-, 0$	$I^+, \pm\frac{\pi}{2}$	0,0	$\frac{B}{\sqrt{3}(V^{-2}-V^{+2})}$
delta	$V^+, 0$	V^-, π	$I^+, \pm\frac{\pi}{2}$	0,0	$\frac{B'}{\sqrt{3}(V^{-2}-V^{+2})}$

Other parameters in Table I are defined as follows:

$$A = \sqrt{C^2(I^- + I^+)^2 + 12(I^- - I^+)^2 P_{\text{disa}}^2}$$

$$A' = \sqrt{C^2(I^- - I^+)^2 + 12(I^- + I^+)^2 P_{\text{disa}}^2}$$

$$B = \sqrt{D^2(V^- + V^+)^2 + 12(V^- - V^+)^2 P_{\text{disa}}^2}$$

$$B' = \sqrt{D^2(V^- - V^+)^2 + 12(V^- + V^+)^2 P_{\text{disa}}^2} \quad (16)$$

with

$$C = 2P_{\text{disa}} + 4P_{\text{disb}} - \sqrt{3}V^+ I^-$$
$$D = 2P_{\text{disa}} + 4P_{\text{disb}} - \sqrt{3}V^- I^+.$$

The solution for the zero-sequence voltage/current shows that a practical limitation exists in both configurations, with an infinite zero-sequence requirement needed under specific operating conditions. In the specific, the operating range of the star configuration is limited by the degree of unbalance (I^-/I^+). From Table I, it can be observed that V_0 tends to infinity when the ratio I^-/I^+ approaches 1, i.e., a theoretically infinite voltage for the Y-point to allow uniform power distribution among phases when the amplitude of the exchanged negative-sequence current equals the amplitude of the positive sequence. In practical applications, the maximum attainable output voltage of the converter leg will determine the maximum degree of unbalance that the converter can cope with before losing the controllability of the dc-link voltages. Similar phenomena will appear for the delta configuration, where the operating range is limited by the degree of voltage unbalance (V^-/V^+). From Table I, it can be observed that the zero-sequence current I_0 tends to infinity when the ratio (V^-/V^+) tends to 1. It is of importance to stress that the singularity is independent from the assumptions in Table I and will occur in any unbalanced condition if the voltage ratio for the delta and the current ratio for the star tends to 1.

Fig. 5 shows the relation between positive- and negative-sequence currents and zero-sequence voltage amplitude for the star configuration when $\delta^+ = \delta^- = \frac{\pi}{2}$ (top) and $\delta^+ = -\delta^- = \frac{\pi}{2}$ (bottom). For the simulated case, V^+ is equal to 1 p.u., while P_{disa} and P_{disb} are set to 0.02 and 0.01 p.u., respectively. Observe that P_{disa}, P_{disb} are intentionally chosen to be very small, since they are introduced to simply model the small disturbances

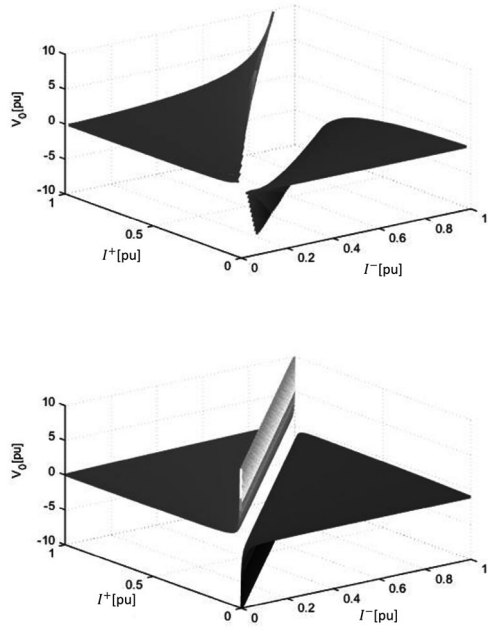

Fig. 5. Relationship between zero-sequence voltage and negative- and positive-sequence currents for star configuration. (top) $\delta^+ = \delta^- = \frac{\pi}{2}$ and (bottom) $\delta^+ = -\delta^- = \frac{\pi}{2}$.

caused by nonidealities. It can be observed that in both operating conditions, the singularity occurs when $I^+ = I^-$. It is of interest to observe that more effort is needed from a balancing point of view (i.e., more zero-sequence voltage injection for the same amount of current unbalance) when the current positive- and negative-sequence components have the same phase angle ($\delta^+ = \delta^- = \frac{\pi}{2}$ in the top figure).

Fig. 6 shows the relation between positive- and negative-sequence voltages and zero-sequence current amplitude for the delta case when $\theta_v^+ = \theta_v^- = 0$ (top) and when $\theta_v^+ = 0, \theta_v^- = \pi$ (bottom). For the simulated case, I^+ is equal to 1 p.u., while P_{disa}, P_{disb} are 0.02 and 0.01 p.u., respectively. It can be observed that in both cases the singularity occurs when $V^+ = V^-$. Similar to the star case, more balancing effort is required when $\theta_v^+ = \theta_v^- = 0$.

It is possible to observe from Figs. 5 and 6 that although star and delta CHB-STATCOMs are sensitive to the degree of unbalanced in the current and voltage, respectively, the required amount of zero-sequence component needed for capacitor balancing also highly depends on the relative phase shift between the sequence components. For this reason, for the star configuration it is of interest to investigate the impact of the relative phase shift between the current sequence components on the required amount of zero-sequence voltage. Analogous investigation can be performed for the delta configuration, where the impact of the relative phase shift between positive- and negative-sequence voltage on the required zero-sequence current is investigated.

Fig. 7, top figure, shows the required zero-sequence voltage as a function of the phase shift between the current sequence components, denoted as ξ_i, and the degree of unbalance in the exchanged current. It is here assumed that the positive-sequence voltage V^+ is equal to 1 p.u. Similar analysis is performed

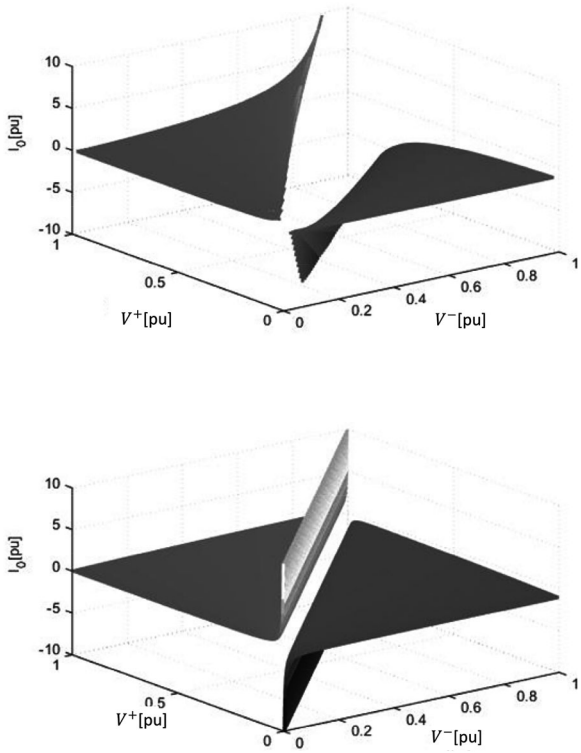

Fig. 6. Relationship between zero-sequence current and negative- and positive-sequence voltages for delta configuration. (top) $\theta_v^+ = \theta_v^- = 0$ (bottom) $\theta_v^+ = 0, \theta_v^- = \pi$.

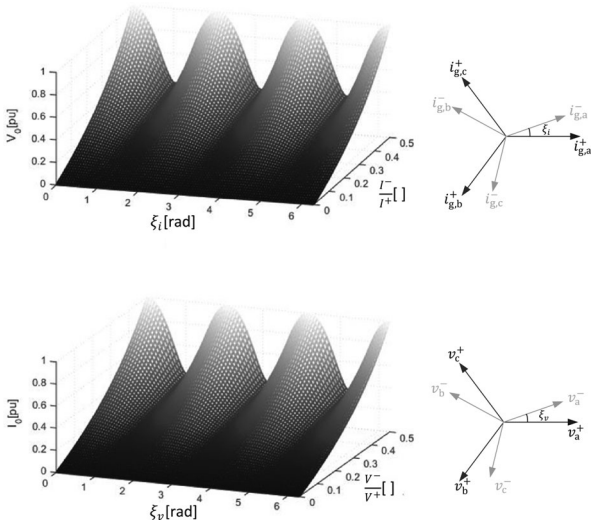

Fig. 7. Impact of phase shift between positive- and negative-sequence component on required zero-sequence component. Top: star configuration; bottom: delta configuration.

for the delta configuration (see Fig. 7, bottom figure), where the impact of the phase shift between the negative- and the positive-sequence voltage is investigated under the assumption that the converter is injecting 1 p.u. positive-sequence current into the grid. Note that the level of unbalance is limited to 0.5 p.u. for clarity of the figure. As shown, the worst case (i.e., highest demand on the zero-sequence component) occurs

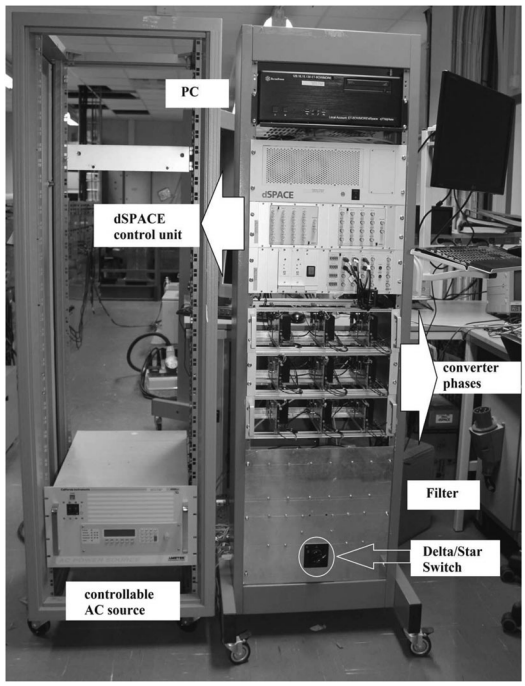

Fig. 8. Photo of the laboratory set up.

when the positive-sequence tern is aligned with the negative-sequence tern (corresponding to $\xi_{i,v} = 0, 2\pi/3, 4\pi/3$); on the contrary, the lowest demand on the zero-sequence component occurs when the two terns are in phase opposition, i.e., for $\xi_{i,v} = \pi/3, \pi, 5\pi/3$. Therefore, it can be concluded that the case studies indicated in Table I where both current sequences are in phase for the star configuration (i.e., $\delta^+ = \delta^- = \pm\frac{\pi}{2}$) or when the voltage sequences are in phase for the delta configuration ($\theta_v^+ = \theta_v^- = 0$) can be seen as the worst case scenarios under the given assumptions.

VI. Experimental Results

The theoretical results obtained in the previous sections are verified through experimental results for both star and delta configuration. A photo of the laboratory set up is shown in Fig. 8, while the system parameters are reported in Table II. The experimental results are focused on the worst-case scenario for both configurations as indicated in the previous section, i.e., $\delta^+ = \delta^- = \pm\frac{\pi}{2}$ for the star and $\theta_v^+ = \theta_v^- = 0$ for the delta.

Fig. 9 shows the obtained experimental results for delta configuration. Fig. 9(a) shows the grid voltage, (b) shows the degree of unbalance in the converter terminal voltage (V^-/V^+), (c) shows the zero-sequence current, and (d) shows the capacitor voltages in all three phases. All quantities are plotted in per unit. The positive-sequence current is set to 0.5 p.u.

As shown in the figure, an increase in the degree of voltage unbalance (V^-/V^+) leads to an increase of the zero-sequence current amplitude, as expected from the investigation carried out in the previous section. ($V^-/V^+ = 1$) is the critical point. If the terms $P_{\rm disa}$ and $P_{\rm disb}$ are neglected, the amplitude of the zero-sequence current in Table I can be simplified to $\frac{I^+V^-}{V^- - V^+}$. It

TABLE II
SYSTEM AND CONTROL PARAMETERS

Rated power	$S_{\rm b}$	1 kVA, 1 p.u.
Rated voltage	$V_{\rm b}$	122.5 V, 1 p.u.
System frequency	$f_{\rm g}$	50 Hz
Filter inductor	L_f	15 mH, 0.23 p.u.
Filter resistor	R_f	1.4 Ω, 0.07 p.u.
Cells capacitor	C	4 mF, 0.05 p.u.
DC-link voltage for star	$V_{\rm dc}$	62 V, 0.5 p.u.
DC-link voltage for delta	$V_{\rm dc}$	106 V, 0.865 p.u.
Cell numbers per phase	n	3
Carrier frequency	$f_{\rm cr}$	3000 Hz
Current control proportional gain	K_p	37.7
Current control integral gain	K_i	3518.5
Overall DC-link proportional gain	$K_{\rm ov}$	0.0065
Cluster control proportional gain	K_z	0.377
Circulating current proportional gain	$K_{\rm i0}$	30
PLL band width	$\alpha_{\rm PLL}$	$2\pi \times 5$ rad/s

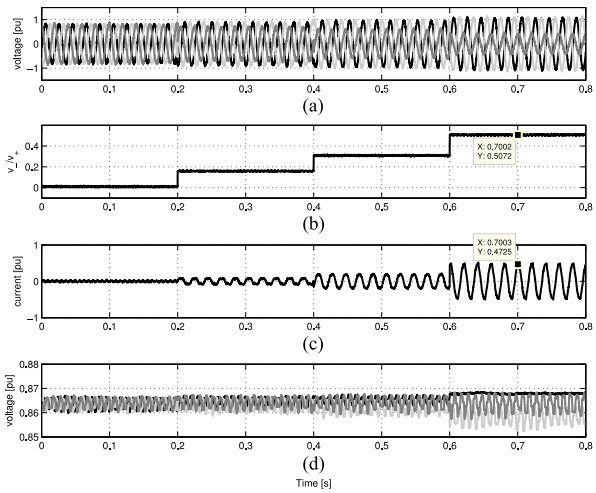

Fig. 9. Experimental results of delta configuration. (a) grid voltage, (b) $\frac{v^-}{v^+}$, (c) zero-sequence current, (d) capacitor voltages.

can be observed from Fig. 9 that, in agreement with the theoretical analysis, for $(V^-/V^+ = 0.5)$ the zero-sequence current is about 0.5 p.u. and equals the amplitude of the positive-sequence current. Observe that an increase in the exchanged positive-sequence current will result in an increase of the zero-sequence current. For example, for the considered level of voltage unbalance, a 1 p.u. positive-sequence current would lead to a 1 p.u. circulating current to guarantee capacitor balancing, meaning that the converter must have a current rating equal to 2 p.u. The required current rating for the converter will further increase if the voltage unbalance is increased. Finally, Fig. 9(d) clearly shows that the implemented control strategy allows proper dc-capacitor voltage balancing.

Fig. 10 shows the obtained experimental results for the star configuration. Fig. 10(a) shows the line current, (b) shows the degree of unbalance in the current injected by the CHB-STATCOM (I^-/I^+), (c) shows the zero-sequence voltage, and (d) shows the capacitor voltages in all three phases. For this experimental study, the line-to-line grid voltage is set to 1 p.u. (corresponding to a peak value of 0.8 p.u. for the line-to-ground voltage) and is perfectly balanced. As expected, an increase in the degree of unbalance in the injected current (I^-/I^+) leads to an increase in amplitude of the zero-sequence voltage V_0, with a singularity when $(I^-/I^+ = 1)$. Note that the implemented controller works properly and is able to keep the capacitor voltages close to the reference value. As for the delta case, neglecting the terms $P_{\rm disa}$ and $P_{\rm disb}$, from Table I the amplitude of the zero-sequence voltage can be simplified to $\frac{I^-V^+}{I^--I^+}$. As it can be observed from Fig. 10, in agreement with the theoretical calculations at $(I^-/I^+ = 0.5)$ a 0.8 p.u. zero-sequence voltage is needed to guarantee capacitor balancing, i.e., a voltage that is equal to the grid voltage. Therefore, for the considered case a 2 p.u. rating in the converter voltage is needed to cope with the considered case. The required voltage rating will further increase if the current unbalance is increased.

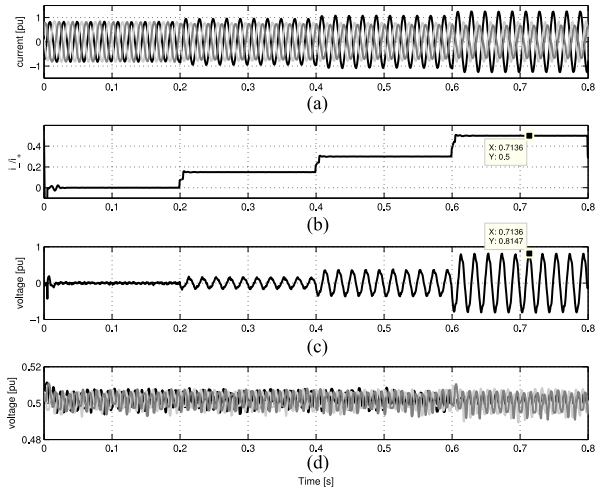

Fig. 10. Experimental results of star configuration. (a) line currents, (b) $\frac{I^-}{I^+}$, (c) zero-sequence voltage, (d), capacitor voltages.

VII. DISCUSSION

The theoretical results provided in this chapter show that under unbalanced conditions there is a limit in the operating range of the CHB-STATCOM, both in star and delta configuration. The star configuration is sensitive to the degree of unbalance in the injected current, while the delta is sensitive to the degree of unbalance in the voltage at the converter terminals. This, together with the specific application, will dictate the selection of the suitable configuration for the CHB-STATCOM and its ratings.

The CHB-STATCOM is mainly used either for utility or industrial applications. Typically, the role of the compensator in utility applications is to regulate the grid voltage at the connection point by aim of positive-sequence current injection. Therefore, for this kind of applications the degree of unbalance in the injected current can be typically considered low, making the star configuration a suitable choice, especially when considering its reduced voltage ratings (thus, reduced number of required cascaded cells) as compared with the delta configuration.

When a STATCOM is employed for industrial applications, instead, its aim is mainly to improve the power quality at the end-user interface, for example to mitigate flicker caused by

arc-furnace load. Under this scenario the compensator must be able to exchange both negative- and positive-sequence currents with the grid and the delta configuration appears as the most preferable choice, especially for systems connected to relatively strong grids. However, it is of importance to stress that this configuration would still suffer from high zero-sequence current requirements in case of asymmetrical faults located in the vicinity of the grid connection point.

VIII. Conclusion

In this chapter, the effect of unbalanced voltage and current on CHB-STATCOM has been investigated, both in case of star and delta configuration of the converter phase legs. Zero-sequence voltage (for the star configuration) or current (delta) allows to maintain the dc-link voltage of the different cells balanced in case of unbalanced operation. However, it has been shown that there are special operating conditions for both the star and the delta configuration where the zero-sequence component is unable to control the active power in each phase to zero. This is due to a singularity that exists in the solution for the calculation of the zero-sequence components. The singularity in the delta configuration occurs when the positive- and negative-sequence components of the voltage at the converter terminals are equal, while for the star case it is governed by the equality between the positive- and the negative-sequence component of the injected current. In addition to the amplitudes, the phase angles of currents in star and voltage in delta will highly impact the sensitivity of the converter. For the star configuration, the highest demand on the zero-sequence voltage occurs when the three-phase positive-sequence currents are aligned with the negative-sequence tern; on the contrary, the lowest demand on the zero-sequence component occurs when the two terns are in phase opposition. Analogue results hold for the delta case. In utility applications, where the priority is on voltage regulation, the converter aims to prioritize positive-sequence current injection to boost the voltage at the connection point and at the same time improve the degree of unbalance. Therefore, the star configuration can be utilized for this purpose. In industrial application, such as arc furnaces, the converter aims to exchange both positive- and negative-sequence current; being this kind of loads typically connected to relatively strong grids, the delta configuration appears the most preferable choice for this kind of applications.

References

[1] C. C. Davidson and G. de Preville, "The future of high power electronics in transmission and distribution power systems," in *Proc. 13th Eur. Conf. Power Electron. Appl.*, Sep. 2009, pp. 1–14.

[2] V. K. Sood, *HVDC and FACTS Controllers—Applications of Static Converters in Power Systems*. Boston, MA, USA: Kluwer, 2004.

[3] H. Akagi, S. Inoue, and T. Yoshii, "Control and performance of a transformerless cascade PWM statcom with star configuration," *IEEE Trans. Ind. Appl.*, vol. 43, no. 4, pp. 1041–1049, Jul. 2007.

[4] J. Yutaka Ota, Y. Shibano, and H. Akagi, "A phase-shifted PWM d-statcom using a modular multilevel cascade converter (SSBC); part II: Zero-voltage-ride-through capability," *IEEE Trans. Ind. Appl.*, vol. 51, no. 1, pp. 289–296, Jan. 2015.

[5] Q. Song and W. Liu, "Control of a cascade statcom with star configuration under unbalanced conditions," *IEEE Trans. Power Electron.*, vol. 24, no. 1, pp. 45–58, Jan. 2009.

[6] N. Hatano and T. Ise, "Control scheme of cascaded h-bridge statcom using zero-sequence voltage and negative-sequence current," *IEEE Trans. Power Del.*, vol. 25, no. 2, pp. 543–550, Apr. 2010.

[7] L. Tan, S. Wang, P. Wang, Y. Li, Q. Ge, H. Ren, and P. Song, "High performance controller with effective voltage balance regulation for a cascade statcom with star configuration under unbalanced conditions," in *Proc. 15th Eur. Conf. Power Electron. Appl.*, Sep. 2013, pp. 1–10.

[8] M. Nieves, J. Maza, J. Mauricio, R. Teodorescu, M. Bongiorno, and P. Rodriguez, "Enhanced control strategy for MMC-based statcom for unbalanced load compensation," in *Proc. 16th Eur. Conf. Power Electron. Appl.*, Aug. 2014, pp. 1–10.

[9] M. Hagiwara, R. Maeda, and H. Akagi, "Negative-sequence reactive-power control by a PWM statcom based on a modular multilevel cascade converter (MMCC-SDBC)," *IEEE Trans. Ind. Appl.*, vol. 48, no. 2, pp. 720–729, Mar. 2012.

[10] R. Betz, T. Summers, and T. Furney, "Symmetry compensation using a h-bridge multilevel statcom with zero sequence injection," in *Proc. 41st Annu. Meeting Ind. Appl. Conf.*, Oct. 2006, vol. 4, pp. 1724–1731.

[11] S. Du, J. Liu, J. Lin, and Y. He, "Control strategy study of statcom based on cascaded PWM h-bridge converter with delta configuration," in *Proc. 7th Int. Power Electron. Motion Control Conf.*, Jun. 2012, vol. 1, pp. 345–350.

[12] H. Akagi, "Classification, terminology, and application of the modular multilevel cascade converter (MMCC)," *IEEE Trans. Power Electron.*, vol. 26, no. 11, pp. 3119–3130, Nov. 2011.

[13] S. Du and J. Liu, "A brief comparison of series-connected modular topology in statcom application," in *Proc. IEEE ECCE Asia Downunder*, Jun. 2013, pp. 456–460.

[14] T. Wijnhoven, G. Deconinck, T. Neumann, and I. Erlich, "Control aspects of the dynamic negative sequence current injection of type 4 wind turbines," in *Proc. IEEE PES General Meeting, Conf. Expo.*, Jul. 2014, pp. 1–5.

[15] R. Betz and T. Summers, "Introduction to symmetrical components and their use in statcom applications," School Electr. Eng. Comput. Sci., Univ. Newcastle, Callaghan, NSW, Australia, Tech. Rep. 0401-02-016.1.9, Nov. 2009.

[16] L. Harnefors and H. Nee, "A general algorithm for speed and position estimation of ac motors," *IEEE Trans. Ind. Electron.*, vol. 47, no. 1, pp. 77–83, Feb. 2000.

[17] O. Wallmark and L. Harnefors, "Sensorless control of salient PMSM drives in the transition region," *IEEE Trans. Ind. Electron.*, vol. 53, no. 4, pp. 1179–1187, Jun. 2006.

[18] J. Svensson and M. B. A. Sannino, "Practical implementation of delayed signal cancellation method for phase-sequence separation," *IEEE Trans. Power Del.*, vol. 22, no. 1, pp. 18–26, Jan. 2007.

[19] L. Harnefors, M. Bongiorno, and S. Lundberg, "Input-admittance calculation and shaping for controlled voltage-source converters," *IEEE Trans. Ind. Electron.*, vol. 54, no. 6, pp. 3323–3334, Dec. 2007.

[20] E. Behrouzian, M. Bongiorno, R. Teodorescu, and J. P. Hasler, "Individual capacitor voltage balancing in h-bridge cascaded multilevel statcom at zero current operating mode," in *Proc. 17th Eur. Conf. Power Electron. Appl.*, Sep. 2015, pp. 1–10.

Ehsan Behrouzian (S'12) received the M.Sc. degree in electrical engineering from the Isfahan University of Technology, Isfahan, Iran, in September 2011. He is currently working toward the Ph.D. degree at the Chalmers University of Technology, Gothenburg, Sweden.

His research interests include application of power electronics in power systems, control theory, and power quality.

Massimo Bongiorno (S'02–M'07–SM'16) received the M.Sc. degree in electrical engineering from the University of Palermo, Palermo, Italy, in April 2002, and the Lic.Eng. and Ph.D. degree from the Chalmers University of Technology, Gothenburg, Sweden, in December 2004 and September 2007, respectively.

From 2007 to 2010, he was an Assistant Professor at the Department of Electric Power Engineering, Chalmers University of Technology, where he became an Associate Professor in 2010. Since 2015, he has been holding the position of Professor in power electronic applications for power systems. His research interests include application of power electronics in power systems, power system dynamics, and power quality.